HHS Public Access

Author manuscript

*Crit Rev Biochem Mol Biol*. Author manuscript; available in PMC 2016 July 01.

Published in final edited form as:

*Crit Rev Biochem Mol Biol*. 2015 ; 51(4): 213–227. doi:10.1080/10409238.2016.1184224.

# Dynamic Structure of Plasma Fibronectin

**Lisa M. Maurer**, **Wenjiang Ma**, and **Deane F. Mosher***

Departments of Biomolecular Chemistry and Medicine, University of Wisconsin-Madison

## Abstract

Fibronectin is a large vertebrate glycoprotein that is found in soluble and insoluble forms and involved in diverse processes. Protomeric fibronectin is a dimer of subunits, each of which comprises 29 to 31 modules—12 type I, two type II, and 15-17 type III. Plasma fibronectin is secreted by hepatocytes and circulates in a compact conformation before it binds to cell surfaces, converts to an extended conformation, and is assembled into fibronectin fibrils. Here we review biophysical and structural studies that have shed light on how plasma fibronectin transitions from the compact to the extended conformation. The three types of modules each have a well-organized secondary and tertiary structure as defined by NMR and crystallography and have been likened to "beads on a string". There are flexible sequences in the N-terminal tail, between the fifth and sixth type I modules, between the first two and last two of the type III modules, and at the C-terminus. Several specific module-module interactions have been identified that likely maintain the compact quaternary structure of circulating fibronectin. The quaternary structure is perturbed in response to binding events, including binding of fibronectin to the surface of vertebrate cells for fibril assembly and to bacterial adhesins.

### Keywords

fibronectin; integrin; plasma protein; bacterial adhesin; syndecan; heparan sulfate; fibronectin type I module; fibronectin type II module; fibronectin type III module

## Introduction

Fibronectin (FN, human gene *FN1*, UniProt entry for human protein: http://www.uniprot.org/uniprot/P02751) is a 470- to 500-kDa glycoprotein of vertebrates that contributes to normal processes important for development, organogenesis, cell adhesion and migration, and hemostasis (George et al., 1993, Pankov and Yamada, 2002, Wang et al., 2014) and pathophysiologic processes such as angiogenesis (Zhou et al., 2008) and vascular remodeling (Chiang et al., 2009). FN has given its name to the three module types that constitute >90% of its sequence: FNI, FNII, and FNIII (Fig. 1). There are two general sources of FN: plasma FN that is synthesized by hepatocytes and secreted into blood where it circulates in a compact conformation and cellular FN that is secreted locally by cells (Tamkun and Hynes, 1983, Moretti et al., 2007). Many of the effects of FN require FN to be

*Contact information: 420 Henry Mall, Madison, WI 53706, Ph: 608 262 1576, dfmosher@wisc.edu.

Declaration of interest: The paper was written by ourselves. We report no conflicts of interest.

assembled into fibrils of the extracellular matrix. FN assembly has been studied mostly in cell culture and involves FN binding to molecules on cell surfaces, including syndecans and integrins, adopting a linear conformation, and recruiting additional FN molecules to form insoluble fibrils (Singh et al., 2010, Fruh et al., 2015). Assembly is initiated at sites of cell adhesion, and growing fibrils are translocated inwards (Pankov et al., 2000, Ohashi et al., 2002).

Plasma FN circulates at 200 to 600 μg $mL^{-1}$ (0.4-1.2 μM) in humans (Zerlauth and Wolf, 1984) and 100 to 400 μg $mL^{-1}$ (0.2-0.8 μM) in mice (Tomasini-Johansson and Mosher, 2009). Remarkably, human plasma FN after purification and concentration is soluble in physiological saline at concentrations (15-20 mg $mL^{1}$ or 30-40 μM) many-fold greater than that found in the circulation (Mosher and Johnson, 1983). Plasma FN is taken up by tissues and deposited in extracellular matrix fibrils alongside locally synthesized cellular FN (Oh et al., 1981, Moretti et al., 2007). The mechanism of *in vivo* deposition is presumed to be mimicked by assembly *in vitro* by cultured fibroblasts, which become competent to assemble plasma FN at low nM concentrations shortly after adhesion to culture dishes (Bae et al., 2004). Plasma FN is also assembled efficiently by adherent platelets in a flow chamber (Cho and Mosher, 2006c). Given the abundance of FN in the plasma, it has long been hypothesized that maintenance of plasma FN in a closed compact conformation is necessary to prevent aberrant interactions among FN protomers and between FN and cell surface receptors and other macromolecules (Pearlstein, 1978, Rocco et al., 1983, Johnson et al., 1999, Singh et al., 2010). Such interactions would be expected to lead to FN assembly in tissues and contribute to thrombus formation in the circulation.

Well before its primary structure was elucidated, purified plasma FN was characterized by a variety of biophysical techniques. The sedimentation velocity and diffusion coefficients were found to decrease as either ionic strength or pH is increased, suggesting that electrostatic interactions maintain FN in its compact conformation (Alexander et al., 1979, Williams et al., 1982, Tooney et al., 1983). Further, light scattering and intrinsic viscosity studies showed that the compact conformation can be perturbed easily inasmuch as the Stoke's radius of FN increased from ∼10.5 nm in ∼150 mM sodium chloride to ∼17.5 nm in ∼1 M sodium chloride (Rocco et al., 1983, Rocco et al., 1987). Rotary shadowing electron microscopy studies visualized FN in compact and V-shape conformations depending on the surface and conditions of adsorption (Odermatt and Engel, 1989). When studies were performed in high salt or acidic or basic conditions, FN had an extended V-shape conformation whereas studies in low salt showed a bent or “irregularly coiled compact” conformation (Tooney et al., 1983, Erickson and Carrell, 1983). On most surfaces, regardless of the conditions tested, there appeared to be a great deal of flexibility along the length of FN (Odermatt and Engel, 1989).

Based on such results and early primary sequence data demonstrating its modular nature, plasma FN was modeled as beads-on-a-string with differences along the string in the degrees that any two beads could bend or rotate relative to one another (Rocco et al., 1983). This model was further developed when the full sequence with its 58 modules (Fig. 1) was known (Rocco et al., 1987). Results of NMR, crystallography, and lower resolution studies are now available that characterize module-module interactions in FN and thus allow one to predict sites of flexibility between modules, shown as arrows in Fig. 1, and long distant interactions

that determine quaternary structure of compact plasma FN (Fig. 2). Here, we work from these studies to arrive at models of the interactions that maintain plasma FN in a compact conformation and how these interactions may be broken and re-arranged in ways that are biological relevant. We pay particular attention to modulation of structure by segments of bacterial surface adhesins that interact specifically with FN.

## Modular make-up of FN and structures of FNI, FNII, and FNIII modules

FN is a dimer of 235-250-kDa subunits. Each subunit is composed of an array of 12 type I (FNI), two FNII, and 15-17 FNIII modules (Fig. 1). We use a nomenclature whereby module type is designated by a Roman number and the positions of the modules of each type, ordered from N- to C-terminus, are designated by superscript Arabic numbers. Dimerization is by a brace of disulfide bonds near the C-termini connecting the two subunits (An et al., 1992).

The variable number of type III modules is a result of differential mRNA splicing that determines inclusion of extra domain A ($^{A}$FNIII) between $^{11}$FNIII and $^{12}$FNIII or extra domain B ($^{B}$FNIII) between $^{7}$FNIII and $^{8}$FNIII (White et al., 2008, Astrof and Hynes, 2009) (Fig. 1). Additionally, differential splicing leads to five different sequences, ranging from 0 to 120 amino acids, that comprise the type III homology connecting segment or V region located between $^{14}$FNIII and $^{15}$FNIII (Muro et al., 2008, Petersen et al., 1989, Hynes, 1990). Random assortment of differential splicing of $^{A}$FNIII, $^{B}$FNIII, and the V region could yield 20 different versions of the human FN subunit and many more possible versions of homodimers and heterodimers. Plasma FN lacks $^{A}$FNIII and $^{B}$FNIII, and one subunit lacks residues in the V region, resulting in a simpler mix of dimers. Mice genetically manipulated to enforce the presence or absence of $^{A}$FNIII and/or $^{B}$FNIII in all FN subunits, including FN in plasma, manifest many abnormalities including changes in fibrosis and thrombosis (White et al., 2008, Astrof and Hynes, 2009). These observations along with biophysical studies of large FN fragments (Johnson et al., 1999) indicate that $^{A}$FNIII and $^{B}$FNIII have important effects on FN structure. However, purified intact FNs harboring $^{A}$FNIII and/or $^{B}$FNIII have been available in only limited quantities (e.g. (Guan et al., 1990, Manabe et al., 1997)) and have not been subjected to the extensive biophysical studies that have been carried out on plasma FN. Thus, this review concentrates on plasma FN alone.

The FNI module is unique to chordates, and the FN protein described above is only present in vertebrates (Tucker and Chiquet-Ehrismann, 2009, Adams et al., 2015). However, the FNI module is related structurally to a submodule within the von Willebrand factor-C module found widely in proteins of chordates and non-chordates, suggesting that FNI modules arose from a von Willebrand factor-C module (O'Leary et al., 2004). FN is the only vertebrate protein with tandem FNI modules. There are single FNI modules in tissue plasminogen activator (PLAT), blood coagulation factor XII (F12), and hepatocyte growth factor activator (HGFAC) (Downing et al., 1992, Smith et al., 1994, Maas et al., 2008). In FN, each FNI module is encoded by a single exon (Hynes, 1990). FNI modules are ∼45 amino acids in length and comprise minor AB and major CDE anti-parallel β-sheets, with conserved Cys1-Cys3 and Cys2-Cys4 disulfides connecting the A and D strands and D and E strands,

respectively (Potts and Campbell, 1996). Ribbon structures of four FNI modules are shown in Fig. 1.

FNII modules are also encoded by individual exons (Hynes, 1990). The modules, both of which are shown in Fig. 1, are ∼60 amino acids in length and comprise two β-sheets that are perpendicular to each other. The majority of the sequence is in loops between strands. Two disulfides are in a Cys1-Cys3/Cys2-Cys4 pattern (Potts and Campbell, 1996, Pickford et al., 1997). Examples of FNII modules are found in matrix metalloproteinases MMP2 and MMP9 (Potts and Campbell, 1996) and other human proteins including F12, HGFAC, BSPH1, ELSPBP1, LY75, IGF2R, MRC1, MRC2, PLA2R1, and SEL1L (http://www.uniprot.org/uniprot/?query=domain%3A%22fibronectin+type+2+domain*%22+AND+human&sort=score).

Two exons encode the majority of FNIII modules of FN whereas single exons encode $^{9}$FNIII, $^{A}$FNIII, and $^{B}$FNIII (Muro et al., 2008, Hynes, 1990). FNIII modules are ∼90 amino acids long, fold into a seven-stranded β-sandwich, and lack disulfide bonds (Potts and Campbell, 1996). Ribbon structures of seven FNIII modules are shown in Fig. 1. FNIII modules are widespread in intracellular as well as extracellular proteins such that UniProt lists >7800 FNIII-module-containing proteins from diverse species, including 322 unique proteins in humans (http://www.uniprot.org/uniprot/?query=domain%3A%22fibronectin+type+3+domain*%22+human&sort=score). In many of these proteins, FNIII modules are present in long arrays, as is the case for FN.

To summarize, FN is a “vertebrate invention” and the only protein with tandem FNI modules and with FNI modules adjacent to a long array of FNIII modules. Other multi-modular extracellular matrix proteins such as laminins, tenascins, and fibrinogen/fibrin do not undergo large conformation changes. The uniqueness of plasma FN, therefore, offers a special challenge in discerning structure-function relationships that account for its ability to deposit in extracellular matrix seemingly at “a drop of a hat” and yet remain soluble at concentrations orders of magnitude greater than the concentrations at which it deposits into extracellular matrix or binds to cell surface receptors.

## Flexible regions within FN

Approximately 90% of the FN sequence can be assigned to FNI, FNII, or FNIII modules. The rest of the sequence (depicted as black lines in Fig. 1) is likely unstructured and flexible (arrows in Fig. 1) as evidenced by NMR spectroscopy or susceptibility to proteolytic cleavage.

Human FN is synthesized with a 31-residue N-terminal “prepro” sequence ending in a consensus furin cleavage sequence (Petersen et al., 1989). The exact site of cleavage within this sequence by signal peptidase upon translocation into the endoplasmic reticulum and contribution of the remaining “pro” sequence to folding and secretion, to our knowledge, have not been approached experimentally. NMR of recombinant protein comprising the 18-residue N-terminal tail and $^{1}$FNI of mature FN indicated that the tail has a mobile random coil structure (Potts et al., 1995). This finding is important because near the tip of the tail are

glutaminyl residues through which FN can be cross-linked to itself or other proteins via ε(γ-glutamyl)-lysine bonds catalyzed by activated blood coagulation Factor XIII and tissue transglutaminase (Hoffmann et al., 2011).

The 28-residue linker between $^{5}$FNI and $^{6}$FNI is much longer than the connectors between other pairs of FNI modules and contains six proline residues. The linking sequence is sensitive to limited proteolysis by trypsin, thrombin, plasmin, or thermolysin, yielding a N-terminal domain comprising five FNI modules (N-$^{5}$FNI) (Pankov and Yamada, 2002). An NMR structure of the $^{1\text{-}2}$FNIII tandem construct showed that $^{2}$FNIII lacks the A-strand, and instead the A-strand is part of a ∼30-residue segment that has the potential to be a flexible connector between the G-strand of $^{1}$FNIII and the B-strand of $^{2}$FNIII (Vakonakis et al., 2007). Although this segment is sensitive to limited proteolysis by thermolysin (Borsi et al., 1986), “end-to-side” interactions between $^{1}$FNIII and $^{2}$FNIII may prevent the two ends of the connector from being mobilized (Vakonakis et al., 2007, Karuri et al., 2009).

The V region, when present, is sensitive to a variety of proteases (Hayashi and Yamada, 1981). Surprisingly, in a crystal structure of $^{12\text{-}15}$FNIII, none of the residues in $^{15}$FNIII were resolved (Sharma et al., 1999). However, $^{15}$FNIII has a buried free cysteine (Smith et al., 1982) and therefore is unlikely to be unstructured. It has been suggested that $^{15}$FNIII lacks residues needed for an A-strand and may use part of the V region for that purpose (Sharma et al., 1999). Finally, there are 32 residues between the C-terminal residue of $^{12}$FNI and the C-terminal inter-subunit disulfides that are likely flexible as evidenced by limited proteolysis experiments with trypsin, chymotrypsin, or plasmin, which produces a 3- to 6-kDa fragment at the C-terminus depending on the enzyme used(An et al., 1992, Pankov and Yamada, 2002).

Differential scanning calorimetry (DSC) has revealed a wide range of melting temperatures for FNIII modules (48°C-121°C) (Litvinovich and Ingham, 1995), and because FNIII modules lack constraining disulfide bonds, it has been hypothesized that strands of FNIII modules can be unfolded under certain conditions (Erickson, 1994). A study looking at exposure of buried cysteines placed by *in vitro* mutagenesis within FNIII modules indicated that in isolation $^{2}$FNIII, $^{3}$FNIII, $^{9}$FNIII, and $^{11}$FNIII unfold (Lemmon et al., 2011). Although FNIII modules in full length FN have not been shown to adopt an unfolded conformation in the circulation, there is substantial computational (Krammer et al., 1999, Paci and Karplus, 1999) and experimental (Lemmon et al., 2011, Baneyx et al., 2001, Baneyx et al., 2002, Smith et al., 2007) evidence that the structure of the FNIII modules can be altered by stretching forces, including those produced by cells during and after FN assembly. It has been suggested that unfolding of FNIII modules explains the observation that with force, the length of FN fibrils can increase 8-fold before 50% of the fibrils break (Ohashi et al., 1999, Klotzsch et al., 2009). Thinking about the additional mobility that could be afforded by unfolding of FNIII modules and how newly mobilized segments might interact with other regions of FN or with other molecules, especially by exchange of the β–strands (Erickson, 1994), is mind-boggling.

Anastellin, truncated $^{1}$FNIII lacking the A and B strands, offers an informative case study of the complexities of unravelling type III modules. This segment of FN was identified as a

chymotryptic fragment that at low concentration partially inhibits deposition of FN into extracellular matrix (Morla and Ruoslahti, 1992) and subsequently studied as a small recombinant protein. The segment attracted considerable interest when it was found to cause aggregation of intact FN when added at high concentration (Morla et al., 1994) and thereby block tumor angiogenesis in mice (the name is derived from “anastello,” Greek for “inhibit” or “force a retreat”) (Yi and Ruoslahti, 2001, Yi et al., 2003) The truncation increases accessibility of the hydrophobic core of $^{1}$FNIII to solvent and causes some of the β–strands to acquire the potential to form backbone hydrogen bonds with β–strands of other proteins (Briknarova et al., 2003). Addition of anastellin to recombinant $^{3}$FNIII makes $^{3}$FNIII more sensitive to cleavage by thermolysin, suggesting that anastellin exposes sequences that are cryptic in intact $^{3}$FNIII (Ohashi et al., 2009). Interestingly, stopped-flow studies indicate that the rate constant for unfolding of $^{3}$FNIII is several orders of magnitude faster than the unfolding rate constants of other FNIII modules (Stine et al., 2015). The unusually fast rate is similar to the independently determined (Ohashi et al., 2009) rate of binding of anastellin to $^{3}$FNIII, consistent with a model in which $^{3}$FNIII has to unfold to interact with anastellin. The interaction of anastellin with $^{3}$FNIII, however, does not totally explain aggregation of FN induced by anastellin because only when $^{2}$FNIII, $^{3}$FNIII, and $^{11}$FNIII were stabilized by engineering disulfides into each was recombinant FN resistant to aggregation induced by anastellin (Ohashi and Erickson, 2011)

## Interactions between adjacent modules

The beads-on-a-string model predicts differences in the degrees with which modules arrayed end-to-end can twist or tilt relative to one another (Rocco et al., 1983). Intrinsic viscosity measurements of plasma FN in its extended conformation at high ionic strength indicated a persistence length of <25 nm, i.e., that the string is quite flexible (Williams et al., 1982). Results of a number of NMR, crystallography, and lower resolution studies are now available that characterize many of the module-module interactions in FN and thus allow one to predict sites of flexibility between modules, shown as arrows in Fig. 1. Importantly, these studies identify regions of FN in which modules are not arrayed end-to-end.

An NMR structure of $^{1\text{-}2}$FNI showed no inter-module interactions suggesting that movement of these modules about the linker is minimally constrained (Potts et al., 1999, Pickford and Campbell, 2004). Two alternate crystal forms and an NMR structure of $^{2}$FNI-$^{3}$FNI were solved that differed in inter-module orientation (Rudino-Pinera et al., 2007). The crystal structures showed buried interfaces between the two modules with the NMR structure being most similar to the crystal structure with the larger buried interface (Rudino-Pinera et al., 2007). A co-crystal of a peptide based on *Staphylococcus aureus* FN-binding adhesin FBPA binding by β-strand addition to consecutive E-strands of $^{2\text{-}3}$FNI (Fig. 1) contained no additional contacts between $^{2}$FNI and $^{3}$FNI (Bingham et al., 2008). There are both NMR and crystal structures of $^{4\text{-}5}$FNI (Bingham et al., 2008, Williams et al., 1994). The NMR structure demonstrated that movement between $^{4}$FNI and $^{5}$FNI is constrained by extensive contacts with $^{5}$FNI of a tryptophan in the C-D loop of $^{4}$FNI (Williams et al., 1994). The tryptophan interactions were also found in the crystal structure of $^{4\text{-}5}$FNI complexed by β-strand addition to a peptide based on FBPA (Bingham et al., 2008). Thus, three of the four potential interfaces between consecutive modules have been examined for the first five FNI

modules and found to exhibit quite different flexibility from one another, large for $^{1-2}$FNI, limited for $^{2-3}$FNI, and none for $^{4-5}$FNI. We are not aware of information pertaining to inter-module contacts between $^{3}$FNI and $^{4}$FNI. The flexibility must allow the five N-terminal FNI modules to adopt a linear conformation with aligned E-strands as evidenced by high affinity binding of unstructured polypeptides based on bacterial adhesins from *Streptococcus pyogenes* that contain motifs for engaging consecutive E-strands of $^{1-5}$FNI by β-strand addition (Marjenberg et al., 2011, Norris et al., 2011, Maurer et al., 2012b). In addition, the spacing between the FNI modules is important for engagement with other proteins as evidenced by an assay in which stretching the inter-modular distances of $^{1-5}$FNI modules decreased the affinity of peptides from *Streptococcus dysgalactiae* or *S. aureus* to $^{1-2}$FNI or $^{4-5}$FNI modules (Chabria et al., 2010).

DSC, intrinsic fluorescence, and NMR indicate that all six modules of the gelatin-binding domain, $^{6-9}$FNI, are independently folded (Litvinovich et al., 1991). Consistently, NMR-deduced structures of $^{1}$FNII (Pickford et al., 1997), $^{2}$FNII (Sticht et al., 1998), and $^{7}$FNI (Baron et al., 1990) demonstrated the expected global fold for each. Further, an NMR structure of $^{1}$FNII-$^{2}$FNII also revealed individual modules with canonical structures and no inter-modular interfaces (Smith et al., 2000). However, when $^{6}$FNI was added to yield $^{6}$FNI-$^{2}$FNII, a hydrophobic interface between $^{6}$FNI and $^{2}$FNII was found that resulted in a compact triangular shape (Pickford et al., 2001). A similar interaction between $^{6}$FNI and $^{2}$FNII was found when $^{7}$FNI was added to yield $^{6-7}$FNI, i.e., a construct comprising $^{6}$FNI, $^{1-2}$FNII, and $^{7}$FNI; interactions also were noted between $^{7}$FNI and $^{1}$FNII-$^{2}$FNII and between $^{1}$FNII and $^{2}$FNII (Erat et al., 2010) (Fig. 1). NMR of the same $^{6-7}$FNI construct complexed to a collagenous peptide demonstrated binding of the peptide to a groove on $^{2}$FNII and extending by β-strand addition to the E-strand of $^{7}$FNI (Erat et al., 2010). The link between $^{7}$FNI and $^{8}$FNI is likely flexible based on small angle x-ray scattering (SAXS) studies of $^{6-9}$FNI without and with binding of the collagenous peptide (Erat et al., 2013). The SAXS studies were interpreted as showing the non-ligated construct in multiple conformations with greater population of the ligated construct in a conformation that has a 90° kink between $^{7}$FNI and $^{8}$FNI modules (Erat et al., 2013). A co-crystal structure of $^{8}$FNI-$^{9}$FNI with peptide based on the α(1) chain of type I collagen showed $^{8}$FNI and $^{9}$FNI as canonical type I modules in a tandem arrangement with a relatively small area buried and the collagenous peptide bound by β-strand addition to $^{8}$FNI (Erat et al., 2009). Putting together the structures of complexes of $^{6-7}$FNI or $^{8-9}$FNI with collagenous peptides, a model of collagen binding to $^{6-9}$FNI was proposed with the binding site comprising the $^{2}$FNII groove and E-strands of $^{7}$FNI and $^{8}$FNI (Erat et al., 2010).

A different structure was found when $^{6-9}$FNI was crystallized in presence of 30-50 mM $Zn^{2+}$ (Graille et al., 2010). The part of the structure comprising $^{6}$FNI-$^{2}$FNII is as described above (Pickford et al., 2001, Erat et al., 2010) and shown in Fig. 1. However, $^{8}$FNI lacks the FNI fold and instead is composed of two long strands that associate with $^{7}$FNI and $^{9}$FN1 to form a large β-sheet structure (Graille et al., 2010). The physiological relevance of the structure in $Zn^{2+}$ is unclear; for instance, the concentrations of $Zn^{2+}$ required for crystallization do not support binding of a collagenous peptide to the gelatin-binding domain (Graille et al., 2010). Further, binding to $^{8-9}$FNI of polypeptides derived from bacterial surface proteins was abolished in the presence of $Zn^{2+}$ (Maurer et al., 2010, Ma et al., 2015a). However, the

radically different structures of $^{8}$FNI within the whole gelatin-binding domain in $Zn^{2+}$ compared to the tandem $^{8-9}$FNI construct indicate that this region in FN has the potential to undergo major conformational rearrangements.

The labile region seemingly extends into $^{9}$FNI$^{1-2}$FNIII. Expression of the epitope of mouse monoclonal antibody L8 requires $^{9}$FNI and $^{1}$FNIII be contiguous (Chernousov et al., 1991). Although the L8 epitope was demonstrated to map to Gln690 of $^{1}$FNIII by in vitro mutagenesis (Maurer et al., 2010), the epitope is sensitive to reduction of disulfides in $^{9}$FNI (Chernousov et al., 1991). These findings indicate that $^{9}$FNI and $^{1}$FNIII share an interface through which the modules influence the structure of one another. $^{1}$FNIII is mechanically weak when subjected to atomic force microscopy compared to $^{1-2}$FNIII, suggesting that $^{1}$FNIII and $^{2}$FNIII also interact (Oberhauser et al., 2002). NMR of $^{2}$FNIII alone revealed that the A-strand is disordered, whereas NMR of $^{1-2}$FNIII was interpreted as showing that the C-terminal end of $^{1}$FNIII is “wedged” along the N-terminal to C-terminal axis of $^{2}$FNIII, creating ∼550-Å$^{2}$ buried interface (Vakonakis et al., 2007). This arrangement involves a twist in the G-strand of $^{2}$FNIII allowed by the absence of a structured A-strand (Vakonakis et al., 2007). The residues from the missing A-strand of $^{2}$FNIII together with 17 residue linking $^{1}$FNIII and $^{2}$FNIII constitute a stretch of ∼30 residues that is unstructured. Consistent with an interaction between $^{1}$FNIII and $^{2}$FNIII, fluorescence resonance energy transfer studies indicated that opposite ends of $^{1}$FNIII and $^{2}$FNIII are within 50-60 Å instead of being extended linearly in opposite directions (Karuri et al., 2009). Mutagenesis studies of the tandem construct implicate a salt bridge between Lys672 in $^{1}$FNIII and Glu767 in $^{2}$FNIII with Lys669 playing a less critical role (Vakonakis et al., 2007, Karuri et al., 2009). It should be noted, however, that studies of a similar but not identical $^{1-2}$FNIII tandem construct failed to demonstrate the inter-module interaction or effects of mutations of putative salt bridge residues (Ohashi and Erickson, 2011). Further, the structure of $^{1-2}$FNIII in the context of neighboring modules, particularly $^{9}$FNI, is not known. Finally, it remains to be determined whether the ∼30 residues are disordered or structured in intact compact or extended FN,

A crystal structure of $^{7}$FNIII-$^{10}$FNIII showed a buried interface of ∼550 Å$^{2}$ between $^{7}$FNIII and $^{8}$FNIII or between $^{8}$FNIII and $^{9}$FNIII and a smaller buried interface of ∼300 Å$^{2}$ between $^{9}$FNIII and $^{10}$FNIII (Leahy et al., 1996). The interface between $^{9}$FNIII and 10FNIII, which is of special interest because deletion of either the arginine-glycine-aspartic acid (RGD) cell adhesive sequence in $^{10}$FNIII or residues of the synergy site in $^{9}$FNIII results in >95% loss of integrin-associated cell adhesion (Obara et al., 1988, Aota et al., 1994), has been analyzed by NMR and other analyses for human (Spitzfaden et al., 1997) and mouse (Copie et al., 1998) $^{9-10}$FNIII. Most of the interactions between $^{9}$FNIII and $^{9}$FNIII were characterized as being of low energy (Spitzfaden et al., 1997). Despite this, correct orientation between the synergy site in $^{9}$FNIII and the RGD in $^{10}$FNIII is required to enhance the interactions of FN with integrins (Grant et al., 1997, Altroff et al., 2004). Addition of residues between $^{9}$FNIII and $^{10}$FNIII, which resulted in increased mobility of the modules as seen by NMR (Spitzfaden et al., 1997), was associated with a decrease in integrin-associated activities, including cell spreading (Grant et al., 1997). However, fixation of the orientation between $^{9}$FNIII and $^{10}$FNIII by introduction of a disulfide bond between the two modules also decreased integrin-associated activities (Altroff et al., 2004).

DSC and fluorescence denaturation experiments showed that $^{12}$FNIII, $^{13}$FNIII, $^{14}$FNIII, and $^{15}$FNIII all fold independently: $^{13}$FNIII was the least stable but appeared to be stabilized by $^{14}$FNIII (Novokhatny et al., 1992). A crystal structure of the V0 variant of $^{12\text{-}15}$FNIII revealed buried interfaces of ∼450 Å$^2$ between $^{12}$FNIII and $^{13}$FNIII and ∼650 Å$^2$ with several charge interactions between $^{13}$FNIII and $^{14}$FNIII (Sharma et al., 1999). None of the residues in $^{15}$FNIII were resolved. As described above, it has been suggested that $^{15}$FNIII lacks residues needed for an A-strand and when possible may use part of the V region for that purpose (Sharma et al., 1999).

With the exception of the three or four extended flexible sequences and the stretch of modules between $^{6}$FNI and $^{2}$FNIII, therefore, when examined the modules in a FN subunit have been arrayed head-to-tail with differences in the freedom of any two consecutive modules to tilt or twist relative to one another. A series of preferential module-module conformations could result in bending. However, it is difficult to predict such bending. For instance, the crystal structures of $^{7\text{-}10}$FNIII and $^{12\text{-}14}$FNIII shown in Fig. 1 exhibited a variety on tilts and twists such that one could envision the string of modules from $^{7}$FNIII to $^{14}$FNIII being anywhere from linear or circular (Sharma et al., 1999). For this reason, module-module interactions seem more likely to be facilitative rather than determinant in allowing plasma FN to adopt a distinct compact quaternary structure.

## Long-range Interactions

Fig. 2 models how long-range interactions could drive plasma FN into a compact structure and when relieved could allow FN to open up and extend. It emphasizes interactions between $^{4}$FNI and $^{3}$FNIII of the same subunit and between $^{2\text{-}3}$FNIII and $^{12\text{-}14}$FNIII of the different subunits.

An NMR titration of FN fragments showed that recombinant $^{4\text{-}5}$FNI interacts with recombinant $^{3}$FNIII with a $K_d$ of 0.15 mM (Vakonakis et al., 2009). This interaction was also studied in recombinant N-$^{3}$FNIII. The interaction appeared to be electrostatic and involve Arg222 in $^{4}$FNI inasmuch as size exclusion chromatography showed that mutation of this residue to alanine caused an increase in the hydrodynamic radius of the recombinant protein (Vakonakis et al., 2009). The $^{4}$FNI-$^{3}$FNIII interaction has possible significance in controlling the migration stimulatory activity of FN in collagen gels. This activity is lacking in intact plasma FN, and among naturally occurring FN splice variants lacking the bulk of the C-terminal modules a FN splice variant comprising N-$^{1}$FNIII has activity whereas the splice variant comprising N-$^{3}$FNIIIl does not (Vakonakis et al., 2009). When the R222A mutation was introduced into $^{4}$FNI of N-$^{3}$FNIII, the construct gained the ability to stimulate fibroblast migration (Vakonakis et al., 2009).

Evidence for interactions involving $^{12\text{-}14}$FNIII comes from studies comparing behavior of solutions with low ionic strength of recombinant FN in which $^{12\text{-}14}$FNIII was deleted or replaced with FNIII domains A1 thru A3 from tenascin C or of large recombinant FN fragments (Johnson et al., 1999). For FN with deletion or replacement of $^{12\text{-}14}$FNIII, lower sedimentation velocities were found than when $^{12\text{-}14}$FNIII was present (Johnson et al., 1999). This finding suggests that $^{12\text{-}14}$FNIII mediates specific interactions that are necessary

to maintain FN in a more compact conformation. Velocity sedimentation experiments using N- and C-terminal truncations of $^{2\text{-}14}$FNIII demonstrated dimerization only in the full-length construct, leading to the conclusion that $^{2\text{-}3}$FNIII from one subunit of FN interacts with $^{12\text{-}14}$FNIII from the other subunit (Johnson et al., 1999).

Fig. 2A, therefore, places $^{3}$FNIII next to $^{4}$FNI within the same subunit and $^{12\text{-}14}$FNIII in one subunit next to $^{2\text{-}3}$FNIII in the opposite subunit, creating two hubs that could drive plasma FN into a distinct compact conformation. The model is supported by immunoassays in which soluble plasma FN is asked to compete for binding of monoclonal antibody III-10 (mAbIII-10) (Ugarova et al., 1995) to FN adsorbed to microtiter plate plastic. mAbIII-10 recognizes $^{10}$FNIII, which contains the RGD cell adhesive sequence for α5β1 and is presumed to be fully exposed when FN is bound to plastic for cell adhesion assays. Competition by soluble plasma FN is poor at physiologic pH and ionic strength (Ugarova et al., 1995), consistent with the known inability of soluble plasma FN to prevent cell adhesion to adsorbed FN (Pearlstein, 1978). Thus, the RGD cell adhesive sequences in the $^{10}$FNIII are depicted as being cryptic in compact plasma FN (Fig. 2A). Removal of $^{1\text{-}5}$FNI from FN or ligation of $^{1\text{-}5}$FNI by β-strand addition greatly increases the recognition of plasma FN by mAbIII-10 (Ensenberger et al., 2004, Maurer et al., 2010, Maurer et al., 2012b). These results suggest that loss of the interaction of $^{4}$FNI with $^{3}$FNIII because $^{4}$FNI is missing or $^{3}$FNIII is displaced by the bacterial adhesin favors unravelling of the compact conformation responsible for the cryptic MAbIII-10 epitope. In addition, pre-incubation of soluble plasma FN with mABIII-10 or heparin increases binding of bacterial adhesins. This finding is consistent with an allosteric network linking binding and conformational change at $^{10}$FNIII or $^{12\text{-}14}$FNIII to binding and conformation of $^{1\text{-}5}$FNI (Maurer et al., 2012b). Rotary shadowing EM images indicated that mAbIII-10 employs its two FAB binding sites to bridge and engage the two subunits of extended adsorbed FN (Ugarova et al., 1995). The EM images raise the possibility that the antigenic epitopes in compact soluble FN are cryptic for two reasons: being buried within a compact conformation and not being separated by a distance that is optimal for bridging. In either case, the manipulations that improve the interaction of mAbIII-10 with intact soluble FN are compatible with unraveling and extension in response to loss of the interactions shown in Fig. 2A.

## Binding of the N-terminal FNI modules to bacteria and disruption of the compact structure of FN

Bacteria have had ∼500 million years to adapt to FN since its “invention” in early vertebrates and seem to have done so with vigor, such that more than 100 different FN-binding bacterial proteins have been identified (Henderson et al., 2011). Many of these belong to the MSCRAMM (microbial surface components recognizing adhesive matrix molecules) family of proteins. MSCRAMMs are common in Gram-positive cocci including *Staphylococcus aureus* and *Streptococcus pyogenes* as well as spirochetes such as *Borrelia burgdorferi*, which causes Lyme disease (Schwarz-Linek et al., 2006). In general these proteins are thought to be involved in bacterial invasion of non-phagocytic host cells (Dziewanowska et al., 1998, Ozeri et al., 1998). MSCRAMMs contain variable numbers of FN binding repeats (FNBRs) with or without non-repetitive upstream or downstream

sequences (Schwarz-Linek et al., 2006). Crystallographic and NMR studies indicate that FNBRs transition from a random coil to bind to the E-strands of consecutive FNI modules via anti-parallel tandem β-strand addition, also called β-zipper formation (Bingham et al., 2008, Schwarz-Linek et al., 2003). An example of such binding for a peptide based on a FNBR that interacts with $^{2-3}$FNI is shown in Fig. 1. The FNBR of the F1 adhesin (allelic variant SfbI) of *S. pyogenes* binds to $^{2-5}$FNI whereas the adjacent downstream non-repetitive domain binds to $^{1}$FNI (Bingham et al., 2008, Schwarz-Linek et al., 2003, Schwarz-Linek et al., 2004). Thus, the binding site for the recombinant polypeptide that we have dubbed HADD (for "high affinity downstream domain") maps to $^{1-5}$FNI (Maurer et al., 2012b) (Fig. 2B). The adjacent upstream non-repetitive domain binds to $^{8-9}$FNI within the gelatin-binding domain of FN (Fig. 2C) (Maurer et al., 2010, Atkin et al., 2010). Mapping and homology modeling studies indicated that binding of FUD ("functional upstream domain"), a 49-amino acid polypeptide comprising the upstream domain and adjacent FNBR of the F1 adhesin, show that FUD binding requires modules $^{6-7}$FNI to "loop-out," i.e., the binding site on fibronectin is discontinuous, jumping from $^{2-5}$FNI to $^{8}$FNI (Maurer et al., 2010) (Fig. 2C). *B. burgdorferi*, which is genetically distant from *S. pyogenes*, encodes the BBK32 adhesin that has a single FN-binding sequence and very different protein organization than the F1 adhesin (Kim et al., 2004). Remarkably, the binding sequence, which we have dubbed Bbk32, also binds to $^{2-5}$FNI and $^{8}$FNI (Harris et al., 2014) (Fig. 2C). As mentioned above, peptides from adhesins in *S. dysgalactiae* and *S. aureus* bind FN less well after FN is stretched (Chabria et al., 2010). This finding suggests that in order to engage the FNBR consecutive FNI modules must have favorable spacing.

Fluorescence polarization stopped-flow assays demonstrated that FUD and Bbk32 bind more rapidly to N-$^{9}$FNI than to FN, likely due to competition for binding from the intramolecular interaction between $^{4}$FNI and $^{3}$FNIII shown in Fig. 2A (Ma et al., 2015b). The on-rates for binding of FUD and Bbk32 to plasma FN were similar, $3.9 \times 10^{5}$ $M^{-1}$ $sec^{-1}$ and $2.9 \times 10^{5} M^{-1}$ $sec^{-1}$, respectively, and ∼10-fold slower than binding of the two probes to N-$^{9}$FNI. The off-rates to either FN or N-$^{9}$FNI, however, were very different, $\sim 3 \times 10^{-2}$ $sec^{-1}$ for Bbk32 and $\ll 10^{-3}$ $sec^{-1}$ for FUD. FUD and Bbk32 differ in the spacing between sequences that interact with $^{3}$FNI and $^{4}$FNI or with $^{5}$FNI and $^{8}$FNI. Thus, it has been suggested that these results indicate a "folding-after-binding" process after initial association of certain polypeptide sequences to FN that results in formation of complexes of variable stability and is a function of sequences between the engagement sites, and perhaps flexibility within the polypeptide-FN complex (Ma et al., 2015b). Thus, even though SfbI and BBK32 adhesins target the same extended binding site on plasma FN, the kinetics of binding are specific for the two adhesins. It has been suggested that bacterial pathogenicity may be determined by stability of adhesin-FN complexes, long-lasting in case of *S. pyogenes* that forms a biofilm in the pharynx and transient for *B. burgdorferi*, which is migratory (Ma et al., 2015b).

Isothermal calorimetric analysis of binding of FN to polypeptides with one or several FNBRs showed that binding of one FN to one FNBR influences FN binding to the adjacent FNBR, i.e., binding of FN to adhesins with multiple FNBRs is cooperative (Marjenberg et al., 2011). It was hypothesized that this binding paradigm would allow a single adhesin to capture and change the conformations of multiple FN dimers, thus exposing multiple RGD motifs that cause integrins to cluster and facilitate cellular invasion by bacteria (Marjenberg

et al., 2011). Of note, strains of *S. aureus* cultured from blood of patients with infected cardiac devices have mutations in the FNBRs of the FNBPA adhesin that increase the strength of binding to FN (Messina et al., 2016)

## Binding of plasma FN to collagen

Deposition of type I and type III collagen into the extracellular matrix in cell culture is dependent on the formation of a FN matrix (Velling et al., 2002, Sottile and Hocking, 2002, Sottile et al., 2007). How FN and collagen interact to form collagen fibrils and the relative importance of this interaction for in vivo collagen fibrillogenesis, however, are obscure (Kadler et al., 2008, Moriya et al., 2011). In fibroblast cultures, FN and type I collagen are found initially in ∼10-nm diameter aperiodic fibrils and later, especially after treatment of cells with ascorbate, in 40-nm diameter fibrils on which FN is present with 70-nm periodicity (Furcht et al., 1980). Thus, two separate types of interactions may take place, first of freshly secreted collagen molecules binding to a polymerized FN fibril, perhaps aligning collagen molecules (Singh et al., 2010), and second of freshly secreted FN molecules associating with sites displayed on fibrils of hydroxylated and polymerized collagen.

As described above, a model combining structural analyses of binding of collagenous peptides to $^{6\text{-}7}$FNI and $^{8\text{-}9}$FNI defines a binding pocket in FN extending from $^{2}$FNII to $^{9}$FNI that is dependent on intramolecular interactions among all six modules ($^{6\text{-}9}$FNI) of the collagen-binding domain (Erat et al., 2010). The model suffers from the fact that the structural studies employed the same sequence from the “3/4 site” of type I or II collagen to probe binding to both $^{2}$FNII-$^{7}$FNI and $^{8\text{-}9}$FNI (Erat et al., 2009, Erat et al., 2010). However, a longer peptide based on residues 70-118 at the “1/10-site” of the $\alpha_2$(I) chain of type I collagen was subsequently demonstrated to use its C-terminal and N-terminal halves specifically to engage $^{2}$FNII-$^{7}$FNI and $^{8\text{-}9}$FNI and increase binding affinity cooperatively (Erat et al., 2013). Thus, type I collagen, with its two $\alpha_1$(I) chains and single $\alpha_2$(I) chain, is proposed to contain multiple sites that bind to the $^{6\text{-}9}$FNI collagen-binding domain with approximately equal micromolar affinity (Erat et al., 2013). One can imagine these sites displayed in collagen fibrils and mediating the periodic binding of FN.

Studies of the R1R2 polypeptide from SFS protein of *Streptococcus equi,* which is a strong inhibitor of FN-collagen binding, revealed a possible mechanism to achieve low nanomolar binding of collagen to FN. R1R2 contains two identical short GxxGE collagen-like repeats and binds to plasma fibronectin via modules $^{8\text{-}9}$FNI in a two-step reaction involving both fibronectin subunits (Ma et al., 2015a). Fig. 2D depicts R1R2 as folding back on itself so as to engage both $^{8}$FNI modules of the FN dimer by anti-parallel β-strand addition. Thus, unlike binding of FUD, HADD, or Bbk32, which is better when isolated N-$^{9}$FNI is targeted (Maurer et al., 2010, Maurer et al., 2012b, Harris et al., 2014), R1R2 binds more tightly to dimeric FN. The two $\alpha_1$(I) and single $\alpha_2$(I) chains of type I collagen are in register and aligned N- to C-terminus (Brodsky and Persikov, 2005). In a soluble system, FN can be cross-linked efficiently to triple-helical type I collagen at 37°C but not at lower temperature (Mosher et al., 1979). At this temperature, there is partial unfolding of collagen at the “3/4 site” in proximity to the GxxGE motif where there is no proline over a stretch of 6 Gxx

triplets (Stultz, 2002, Leikina et al., 2002, An et al., 2014). FN may mimic binding to the two repeats of R1R2 by associating with locally denatured sequences of two of the three subunits of type I collagen in a high affinity interaction (Ma et al., 2015a). A key consequence of this model is that for assembled FN to bind to, and possibly facilitate assembly of, nascent type I collagen, the two $^{8}$FNI modules must remain in proximity after incorporation of FN into extracellular matrix (Fig. 2D). Consistent with this notion, imaging studies employing fluorescence probes as an indicator of strain exerted on FN fibrils indicate that collagen associates preferentially with relaxed fibrils, as freshly elaborated FN fibrils are known to be (Kubow et al., 2015)

## Assembly of plasma FN

Assembly of plasma FN requires that the protein becomes extended. There are two proposed ways to initiate extension: interaction of the N-terminal 70-kDa region of FN comprising N-$^{9}$FNI with the cell surface (Tomasini-Johansson et al., 2006) and interaction of the integrin-binding RGD motif in $^{10}$FNIII with cell surface integrins (Geiger et al., 2001). Several pieces of evidence support initiation of FN assembly by binding of N-$^{9}$FNI to cell-surface molecules. The presence of N-$^{5}$FNI is essential for FN assembly (Schwarzbauer, 1991, Takahashi et al., 2007), isolated N-$^{9}$FNI binds to the cell-surface with the same kinetics as full-length FN (Zhang et al., 1994, Cho and Mosher, 2006a), N-$^{9}$FNI is a dominant negative inhibitor of FN assembly (McKeown-Longo and Mosher, 1985), and polypeptides such as FUD that bind to the 70K region block FN assembly (Tomasini-Johansson et al., 2001, Cho and Mosher, 2006b).

Cell-surface receptors for N-$^{9}$FNI remain unknown. There are potential integrin-binding sites in N-$^{9}$FNI, namely NGR motifs that spontaneously convert to integrin binding *iso*DGR motifs (Curnis et al., 2006), and IGD motifs, which stimulate fibroblast migration into type I collagen gels (Schor et al., 1999, Millard et al., 2007). However, neither the NGR motifs nor IGD motifs are required for binding of N-$^{9}$FNI to the cell surface sites of assembly (Xu et al., 2010, Maurer et al., 2012a). N-$^{9}$FNI appears to bind to the cell surface via multiple FNI modules as evidenced by studies showing that deletion of single FNI modules in N-$^{5}$FNI destroys binding of N-$^{9}$FNI to the cell surface (Sottile et al., 1991). Attempts to identify cell-surface binding partners of N-$^{9}$FNI by photo-affinity cross-linking have identified only very large molecules (Zhang and Mosher, 1996). Such attempts need to be re-assessed knowing that N-$^{9}$FNI can be engaged by rapid-on, rapid-off ligands such as Bbk32. When interactors of N-$^{9}$FNI in plasma or platelet lysates were isolated by IFAST (immiscible filtration assisted by surface tension) in which bound molecules are separated from free by rapid passage through an immiscible barrier so as to capture transient binding, 36 interactors were identified by mass spectrometry, 31 in plasma and five in platelet lysate, of which only eight were previously known to interact with FN (Moussavi-Harami et al., 2013). The interactions were all specific as defined by blocking with FUD and therefore likely involve N-$^{9}$FNI binding by β-strand addition to an intrinsically disordered region of the interactor. Disordered regions are common throughout the proteome and well-known mediators of protein-protein interactions (e.g. (Tompa et al., 2015)), and it seems likely that segments of multiple cell surface molecules mimic Bbk32 and interact transiently with the N-$^{9}$FNI region of FN. Whether such interactions are productive of assembly may depend on whether

the interactions coincide with other transient interactions such as unfolding of $^{3}$FNIII (Stine et al., 2015) or binding of α5β1 integrin to $^{10}$FNIII (Takagi et al., 2003).

To understand FN assembly further, one would like to know the molecular architecture of FN in fibrils, i.e., which parts of FN interact with one another. Fig. 2E is based on the concluding figure in a recent examination of native fibronectin fibrils by site-specific protein labelling and single-molecule localization by stepwise photobleaching or direct stochastic optical reconstruction microscopy (Fruh et al., 2015). Single end-labelled fibronectin molecules had an average end-to-end distance of 133 nm, and antibody epitopes displayed periodic punctate label patterns with ∼95 nm repeats and alternating N- and C-terminal regions. These measurements suggested an antiparallel 30-40 nm overlap between N-termini. Thus, the first five type I modules are depicted as binding type III modules of the adjacent molecule, in a sense reversing the interactions in compact FN proposed in Fig. 2A. However, exactly which modules interact with which and the nature of the interactions—β-strand addition, β-strand invasion and exchange, complementary surfaces of folded modules finding one another—remain obscure.

## Concluding remarks

Research over the last several decades has greatly increased our understanding of the structures of the FNI, FNII, and FNIII modules that compose FN and of how certain of these modules array themselves within plasma FN. Here, we work from this progress to understand plasma FN itself. The models of plasma FN in its compact form and how the compact form can open up, although based on a coherent set of experimental observations, are speculative and offered to catalyze further thinking. Much needs to be learned. For instance, when and how does plasma FN adopt the compact form during biosynthesis? Is the propeptide important for adopting the form? How does FN avoid binding to the many potential interacting molecules in the secretory pathway, i.e., are there specific chaperones? Most of this review concentrates on the N-terminal part of the FN subunit. Do the FNI and FNIII modules near the C-terminus have similar susceptibility to conformational change and what is their structure and function? The review, to maintain focus, does not discuss the structural and functional consequences of introducing $^{A}$FNIII and $^{B}$FNIII into FN. These consequences are important and need to be understood. Advances in proteomics, imaging, and single molecule analysis should make it possible to address such issues and questions.

## Acknowledgments

We thank our many colleagues for stimulating conversations and input.

## References

Adams JC, Chiquet-Ehrismann R, Tucker RP. The evolution of tenascins and fibronectin. Cell Adh Migr. 2015; 9:22–33. [PubMed: 25482621]

Alexander SS JR, Colonna G, Edelhoch H. The structure and stability of human plasma cold-insoluble globulin. The Journal of biological chemistry. 1979; 254:1501–5. [PubMed: 762148]

Altroff H, Schlinkert R, Van Der Walle CF, Bernini A, Campbell ID, Werner JM, Mardon HJ. Interdomain tilt angle determines integrin-dependent function of the ninth and tenth FIII domains of

human fibronectin. The Journal of biological chemistry. 2004; 279:55995–6003. [PubMed: 15485890]

An B, Abbonante V, Yigit S, Balduini A, Kaplan DL, Brodsky B. Definition of the native and denatured type II collagen binding site for fibronectin using a recombinant collagen system. The Journal of biological chemistry. 2014; 289:4941–51. [PubMed: 24375478]

An SS, Jimenez-Barbero J, Petersen TE, Llinas M. The two polypeptide chains in fibronectin are joined in antiparallel fashion: NMR structural characterization. Biochemistry. 1992; 31:9927–33. [PubMed: 1390775]

Aota S, Nomizu M, Yamada KM. The short amino acid sequence Pro-His-Ser-Arg-Asn in human fibronectin enhances cell-adhesive function. The Journal of biological chemistry. 1994; 269:24756–61. [PubMed: 7929152]

Astrof S, Hynes RO. Fibronectins in vascular morphogenesis. Angiogenesis. 2009; 12:165–75. [PubMed: 19219555]

Atkin KE, Brentnall AS, Harris G, Bingham RJ, Erat MC, Millard CJ, Schwarz-Linek U, Staunton D, Vakonakis I, Campbell ID, Potts JR. The streptococcal binding site in the gelatin-binding domain of fibronectin is consistent with a non-linear arrangement of modules. The Journal of biological chemistry. 2010; 285:36977–83. [PubMed: 20843804]

Bae E, Sakai T, Mosher DF. Assembly of exogenous fibronectin by fibronectin-null cells is dependent on the adhesive substrate. J Biol Chem. 2004; 279:35749–59. [PubMed: 15199047]

Baneyx G, Baugh L, Vogel V. Coexisting conformations of fibronectin in cell culture imaged using fluorescence resonance energy transfer. Proc Natl Acad Sci USA. 2001; 98:14464–8. [PubMed: 11717404]

Baneyx G, Baugh L, Vogel V. Fibronectin extension and unfolding within cell matrix fibrils controlled by cytoskeletal tension. Proc Natl Acad Sci USA. 2002; 99:5139–43. [PubMed: 11959962]

Baron M, Norman D, Willis A, Campbell LD. Structure of the fibronectin type 1 module. Nature. 1990; 345:642–646. [PubMed: 2112232]

Bingham RJ, Rudino-Pinera E, Meenan NA, Schwarz-Linek U, Turkenburg JP, Hook M, Garman EF, Potts JR. Crystal structures of fibronectin-binding sites from Staphylococcus aureus FnBPA in complex with fibronectin domains. Proceedings of the National Academy of Sciences of the United States of America. 2008; 105:12254–8. [PubMed: 18713862]

Borsi L, Castellani P, Balza E, Siri A, Pellecchia C, De Scalzi F, Zardi L. Large-scale procedure for the purification of fibronectin domains. Analytical biochemistry. 1986; 155:335–45. [PubMed: 3728983]

Briknarova K, Akerman ME, Hoyt DW, Ruoslahti E, Ely KR. Anastellin, an FN3 fragment with fibronectin polymerization activity, resembles amyloid fibril precursors. J Mol Biol. 2003; 332:205–15. [PubMed: 12946358]

Brodsky B, Persikov AV. Molecular structure of the collagen triple helix. Advances in protein chemistry. 2005; 70:301–39. [PubMed: 15837519]

Chabria M, Hertig S, Smith ML, Vogel V. Stretching fibronectin fibres disrupts binding of bacterial adhesins by physically destroying an epitope. Nature communications. 2010; 1:135.

Chernousov MA, Fogerty FJ, Koteliansky VE, Mosher DF. Role of the I-9 and III-1 modules of fibronectin in formation of an extracellular fibronectin matrix. J Biol Chem. 1991; 266:10851–10858. [PubMed: 1710215]

Chiang HY, Korshunov VA, Serour A, Shi F, Sottile J. Fibronectin is an important regulator of flow-induced vascular remodeling. Arterioscler Thromb Vasc Biol. 2009; 29:1074–9. [PubMed: 19407246]

Cho J, Mosher DF. Characterization of fibronectin assembly by platelets adherent to adsorbed laminin-111. J Thromb Haemost. 2006a; 4:943–51. [PubMed: 16689739]

Cho J, Mosher DF. Enhancement of thrombogenesis by plasma fibronectin cross-linked to fibrin and assembled in platelet thrombi. Blood. 2006b; 107:3555–63. [PubMed: 16391013]

Cho J, Mosher DF. Role of fibronectin assembly in platelet thrombus formation. J Thromb Haemost. 2006c; 4:1461–9. [PubMed: 16839338]

Copie V, Tomita Y, Akiyama SK, Aota SI, Yamada KM, Venable RM, Pastor RW, Krueger S, Torchia DA. Solution structure and dynamics of linked cell attachment modules of mouse fibronectin

containing the RGD and synergy regions: comparison with the human fibronectin crystal structure. J Mol Biol. 1998; 277:663–682. [PubMed: 9533887]

Curnis F, Longhi R, Crippa L, Cattaneo A, Dondossola E, Bachi A, Corti A. Spontaneous formation of L-isoaspartate and gain of function in fibronectin. J Biol Chem. 2006; 281:36466–76. [PubMed: 17015452]

Downing AK, Driscoll PC, Harvey TS, Dudgeon TJ, Smith BO, Baron M, Campbell ID. Solution structure of the fibrin binding finger domain of tissue-type plasminogen activator determined by 1H nuclear magnetic resonance. J Mol Biol. 1992; 225:821–33. [PubMed: 1602484]

Dziewanowska K, Patti JM, Deobald CF, Bayles KW, Trumble WR, Bohach GA. Fibronectin Binding Protein and Host Cell Tyrosine Kinase are Required for Internalization of Staphylococcus aureus by Epithelial Cells. Infect Immun. 1998; 67:4673–4678. [PubMed: 10456915]

Ensenberger MG, Annis DS, Mosher DF. Actions of the functional upstream domain of protein F1 of Streptococcus pyogenes on the conformation of fibronectin. Biophys Chem. 2004; 112:201–7. [PubMed: 15572249]

Erat MC, Schwarz-Linek U, Pickford AR, Farndale RW, Campbell ID, Vakonakis I. Implications for collagen binding from the crystallographic structure of fibronectin 6FnI1-2FnII7FnI. The Journal of biological chemistry. 2010; 285:33764–70. [PubMed: 20739283]

Erat MC, Sladek B, Campbell ID, Vakonakis I. Structural analysis of collagen type I interactions with human fibronectin reveals a cooperative binding mode. The Journal of biological chemistry. 2013; 288:17441–50. [PubMed: 23653354]

Erat MC, Slatter DA, Lowe ED, Millard CJ, Farndale RW, Campbell ID, Vakonakis I. Identification and structural analysis of type I collagen sites in complex with fibronectin fragments. Proceedings of the National Academy of Sciences of the United States of America. 2009; 106:4195–200. [PubMed: 19251642]

Erickson HP. Reversible unfolding of fibronectin type III and immunoglobulin domains provides the structural basis for stretch and elasticity of titin and fibronectin. Proc Natl Acad Sci USA. 1994; 91:10114–10118. [PubMed: 7937847]

Erickson HP, Carrell NA. Fibronectin in extended and compact conformations. Electron microscopy and sedimentation analysis. J Biol Chem. 1983; 258:14539–44. [PubMed: 6643500]

Fruh SM, Schoen I, Ries J, Vogel V. Molecular architecture of native fibronectin fibrils. Nature communications. 2015; 6:7275.

Furcht LT, Smith D, Wendelschafer-Crabb G, Mosher DF, Foidart JM. Fibronectin presence in native collagen fibrils of human fibroblasts: Immunoperoxidase and immunoferritin localization. J Histo Cyto. 1980; 28:1319–1333.

Geiger B, Bershadsky A, Pankov R, Yamada KM. Transmembrane crosstalk between the extracellular matrix--cytoskeleton crosstalk. Nat Rev Mol Cell Biol. 2001; 2:793–805. [PubMed: 11715046]

George EL, Georges-Labouesse EN, Patel-King RS, Rayburn H, Hynes RO. Defects in mesoderm, neural tube and vascular development in mouse embryos lacking fibronectin. Development. 1993; 119:1079–1091. [PubMed: 8306876]

Graille M, Pagano M, Rose T, Ravaux MR, Van Tilbeurgh H. Zinc induces structural reorganization of gelatin binding domain from human fibronectin and affects collagen binding. Structure. 2010; 18:710–8. [PubMed: 20541508]

Grant RP, Spitzfaden C, Altroff H, Campbell ID, Mardon HJ. Structural requirements for biological activity of the ninth and tenth FIII domains of human fibronectin. The Journal of biological chemistry. 1997; 272:6159–66. [PubMed: 9045628]

Guan JL, Trevithick JE, Hynes RO. Retroviral expression of alternatively spliced forms of rat fibronectin. J Cell Biol. 1990; 110:833–847. [PubMed: 2307710]

Harris G, Ma W, Maurer LM, Potts JR, Mosher DF. Borrelia burgdorferi protein BBK32 binds to soluble fibronectin via the N-terminal 70-kDa region, causing fibronectin to undergo conformational extension. The Journal of biological chemistry. 2014; 289:22490–9. [PubMed: 24962582]

Hayashi M, Yamada KM. Differences in domain structures between plasma and cellular fibronectins. J Biol Chem. 1981; 256:11292–300. [PubMed: 7287767]

Henderson B, Nair S, Pallas J, Williams MA. Fibronectin: a multidomain host adhesin targeted by bacterial fibronectin-binding proteins. FEMS microbiology reviews. 2011; 35:147–200. [PubMed: 20695902]

Hoffmann BR, Annis DS, Mosher DF. Reactivity of the N-terminal region of fibronectin protein to transglutaminase 2 and factor XIIIA. The Journal of biological chemistry. 2011; 286:32220–30. [PubMed: 21757696]

Hynes, RO. Fibronectins. New York: Springer-Verlag, Inc; 1990.

Johnson KJ, Sage H, Briscoe G, Erickson HP. The compact conformation of fibronectin is determined by intramolecular ionic interactions. J Biol Chem. 1999; 274:15473–15479. [PubMed: 10336438]

Kadler KE, Hill A, Canty-Laird EG. Collagen fibrillogenesis: fibronectin, integrins, and minor collagens as organizers and nucleators. Current opinion in cell biology. 2008; 20:495–501. [PubMed: 18640274]

Karuri NW, Lin Z, Rye HS, Schwarzbauer JE. Probing the conformation of the fibronectin III1-2 domain by fluorescence resonance energy transfer. The Journal of biological chemistry. 2009; 284:3445–52. [PubMed: 19064996]

Kim JH, Singvall J, Schwarz-Linek U, Johnson BJ, Potts JR, Hook M. BBK32, a fibronectin binding MSCRAMM from Borrelia burgdorferi, contains a disordered region that undergoes a conformational change on ligand binding. J Biol Chem. 2004; 279:41706–14. [PubMed: 15292204]

Klotzsch E, Smith ML, Kubow KE, Muntwyler S, Little WC, Beyeler F, Gourdon D, Nelson BJ, Vogel V. Fibronectin forms the most extensible biological fibers displaying switchable force-exposed cryptic binding sites. Proc Natl Acad Sci USA. 2009; 106:18267–72. [PubMed: 19826086]

Krammer A, Lu H, Isralewitz B, Schulten K, Vogel V. Forced unfolding of the fibronectin type III module reveals a tensile molecular recognition switch. Proc Natl Acad Sci USA. 1999; 96:1351–6. [PubMed: 9990027]

Kubow KE, Vukmirovic R, Zhe L, Klotzsch E, Smith ML, Gourdon D, Luna S, Vogel V. Mechanical forces regulate the interactions of fibronectin and collagen I in extracellular matrix. Nature communications. 2015; 6:8026.

Leahy DJ, Aukhil I, Erickson HP. 2.0 Å crystal structure of a four-domain segment of human fibronectin encompassing the RGD loop and synergy region. Cell. 1996; 84:155–164. [PubMed: 8548820]

Leikina E, Mertts MV, Kuznetsova N, Leikin S. Type I collagen is thermally unstable at body temperature. Proceedings of the National Academy of Sciences of the United States of America. 2002; 99:1314–8. [PubMed: 11805290]

Lemmon CA, Ohashi T, Erickson HP. Probing the folded state of fibronectin type III domains in stretched fibrils by measuring buried cysteine accessibility. J Biol Chem. 2011; 286:26375–82. [PubMed: 21652701]

Litvinovich SV, Ingham KD. Interactions between type III domains in the 110 kDa cell-binding fragment of fibronectin. J Mol Biol. 1995; 248:611–626. [PubMed: 7752228]

Litvinovich SV, Strickland DK, Medved LV, Ingham KC. Domain structure and interactions of the type I and type II modules in the gelatin-binding region of fibronectin. J Mol Biol. 1991; 217:563–575. [PubMed: 1994038]

Ma W, Ma H, Fogerty FJ, Mosher DF. Bivalent ligation of the collagen-binding modules of fibronectin by SFS, a non-anchored bacterial protein of Streptococcus equi. The Journal of biological chemistry. 2015a; 290:4866–76. [PubMed: 25525266]

Ma W, Ma H, Mosher DF. On-Off Kinetics of Engagement of FNI Modules of Soluble Fibronectin by beta-Strand Addition. PloS one. 2015b; 10:e0124941. [PubMed: 25919138]

Maas C, Schiks B, Strangi RD, Hackeng TM, Bouma BN, Gebbink MF, Bouma B. Identification of fibronectin type I domains as amyloid-binding modules on tissue-type plasminogen activator and three homologs. Amyloid. 2008; 15:166–80. [PubMed: 18925455]

Manabe R, Ohe N, Maeda T, Fukuda T, Sekiguchi K. Modulation of cell-adhesive activity of fibronectin by the alternatively spliced EDA segment. The Journal of cell biology. 1997; 139:295–307. [PubMed: 9314547]

Marjenberg ZR, Ellis IR, Hagan RM, Prabhakaran S, Hook M, Talay SR, Potts JR, Staunton D, Schwarz-Linek U. Cooperative binding and activation of fibronectin by a bacterial surface protein. J Biol Chem. 2011; 286:1884–94. [PubMed: 21059652]

Maurer LM, Annis DS, Mosher DF. IGD motifs, which are required for migration stimulatory activity of fibronectin type I modules, do not mediate binding in matrix assembly. PloS one. 2012a; 7:e30615. [PubMed: 22355321]

Maurer LM, Ma W, Eickstaedt NL, Johnson IA, Tomasini-Johansson BR, Annis DS, Mosher DF. Ligation of the fibrin-binding domain by beta-strand addition is sufficient for expansion of soluble fibronectin. The Journal of biological chemistry. 2012b; 287:13303–12. [PubMed: 22351755]

Maurer LM, Tomasini-Johansson BR, Ma W, Annis DS, Eickstaedt NL, Ensenberger MG, Satyshur KA, Mosher DF. Extended binding site on fibronectin for the functional upstream domain of protein F1 of Streptococcus pyogenes. J Biol Chem. 2010; 285:41087–99. [PubMed: 20947497]

Mckeown-Longo PJ, Mosher DF. Interaction of the 70,000-mol-wt amino-terminal fragment of fibronectin with the matrix-assembly receptor of fibroblasts. J Cell Biol. 1985; 100:364–374. [PubMed: 3155749]

Messina JA, Thaden JT, Sharma-Kuinkel BK, Fowler VG JR. Impact of Bacterial and Human Genetic Variation on Staphylococcus aureus Infections. PLoS pathogens. 2016; 12:e1005330. [PubMed: 26766507]

Millard CJ, Ellis IR, Pickford AR, Schor AM, Schor SL, Campbell ID. The role of the fibronectin IGD motif in stimulating fibroblast migration. J Biol Chem. 2007; 282:35530–5. [PubMed: 17921136]

Moretti FA, Chauhan AK, Iaconcig A, Porro F, Baralle FE, Muro AF. A major fraction of fibronectin present in the extracellular matrix of tissues is plasma-derived. J Biol Chem. 2007; 282:28057–62. [PubMed: 17644525]

Moriya K, Bae E, Honda K, Sakai K, Sakaguchi T, Tsujimoto I, Kamisoyama H, Keene DR, Sasaki T, Sakai T. A fibronectin-independent mechanism of collagen fibrillogenesis in adult liver remodeling. Gastroenterology. 2011; 140:1653–63. [PubMed: 21320502]

Morla A, Ruoslahti E. A fibronectin self-assembly site involved in fibronectin matrix assembly: reconstruction in a synthetic peptide. J Cell Biol. 1992; 118:421–429. [PubMed: 1629240]

Morla A, Zhang Z, Ruoslahti E. Superfibronectin is a functionally distinct form of fibronectin. Nature. 1994; 367:193–196. [PubMed: 8114919]

Mosher DF, Johnson RB. *In* vitro formation of disulfide-bonded fibronectin multimers. J Biol Chem. 1983; 10:6595–6601. [PubMed: 6133865]

Mosher DF, Schad PE, Kleinman HK. Cross-linking of fibronectin to collagen by blood coagulation factor XIIIa. J Clin Invest. 1979; 64:781–787. [PubMed: 38260]

Moussavi-Harami SF, Annis DS, Ma W, Berry SM, Coughlin EE, Strotman LN, Maurer LM, Westphall MS, Coon JJ, Mosher DF, Beebe DJ. Characterization of molecules binding to the 70K N-terminal region of fibronectin by IFAST purification coupled with mass spectrometry. Journal of proteome research. 2013; 12:3393–404. [PubMed: 23750785]

Muro AF, Moretti FA, Moore BB, Yan M, Atrasz RG, Wilke CA, Flaherty KR, Martinez FJ, Tsui JL, Sheppard D, Baralle FE, Toews GB, White ES. An essential role for fibronectin extra type III domain A in pulmonary fibrosis. Am J Respir Crit Care Med. 2008; 177:638–45. [PubMed: 18096707]

Norris NC, Bingham RJ, Harris G, Speakman A, Jones RP, Leech A, Turkenburg JP, Potts JR. Structural and functional analysis of the tandem beta-zipper interaction of a Streptococcal protein with human fibronectin. The Journal of biological chemistry. 2011; 286:38311–20. [PubMed: 21840989]

Novokhatny V, Schwarz F, Atha D, Ingham K. Domain structure and domain-domain interactions in the carboxy-terminal heparin binding region of fibronectin. Journal of molecular biology. 1992; 227:1182–91. [PubMed: 1433292]

O'leary JM, Hamilton JM, Deane CM, Valeyev NV, Sandell LJ, Downing AK. Solution structure and dynamics of a prototypical chordin-like cysteine-rich repeat (von Willebrand Factor type C module) from collagen IIA. J Biol Chem. 2004; 279:53857–66. [PubMed: 15466413]

Obara M, Kang MS, Yamada KM. Site-directed mutagenesis of the cell-binding domain of human fibronectin: separable, synergistic sites mediate adhesive function. Cell. 1988; 53:649–657. [PubMed: 3286012]

Oberhauser AF, Badilla-Fernandez C, Carrion-Vazquez M, Fernandez JM. The mechanical hierarchies of fibronectin observed with single-molecule AFM. Journal of molecular biology. 2002; 319:433–47. [PubMed: 12051919]

Odermatt, E.; Engel, J. Physical properties of fibronectin. In: Mosher, DF., editor. Fibronectin. New York: Academic Press; 1989.

Oh E, Pierschbacher M, Ruoslahti E. Deposition of plasma fibronectin in tissues. Proc Natl Acad Sci USA. 1981; 78:3218–3221. [PubMed: 6789333]

Ohashi T, Augustus AM, Erickson HP. Transient opening of fibronectin type III (FNIII) domains: the interaction of the third FNIII domain of FN with anastellin. Biochemistry. 2009; 48:4189–97. [PubMed: 19320499]

Ohashi T, Erickson HP. Fibronectin aggregation and assembly: the unfolding of the second fibronectin type III domain. The Journal of biological chemistry. 2011; 286:39188–99. [PubMed: 21949131]

Ohashi T, Kiehart DP, Erickson HP. Dynamics and elasticity of the fibronectin matrix in living cell culture visualized by fibronectin-green fluorescent protein. Proc Natl Acad Sci U S A. 1999; 96:2153–2158. [PubMed: 10051610]

Ohashi T, Kiehart DP, Erickson HP. Dual labeling of the fibronectin matrix and actin cytoskeleton with green fluorescent protein variants. J Cell Sci. 2002; 115:1221–9. [PubMed: 11884521]

Ozeri V, Rosenshine I, Mosher DF, Fassler R, Hanski E. Roles of integrins and fibronectin in the entry of Streptococcus pyogenes into cells via protein F1. Mol Microbiol. 1998; 30:625–37. [PubMed: 9822827]

Paci E, Karplus M. Forced unfolding of fibronectin type 3 modules: an analysis by biased molecular dynamics simulations. J Mol Biol. 1999; 288:441–59. [PubMed: 10329153]

Pankov R, Cukierman E, Katz BZ, Matsumoto K, Lin DC, Lin S, Hahn C, Yamada KM. Integrin dynamics and matrix assembly: tensin-dependent translocation of alpha(5)beta(1) integrins promotes early fibronectin fibrillogenesis. J Cell Biol. 2000; 148:1075–90. [PubMed: 10704455]

Pankov R, Yamada KM. Fibronectin at a glance. J Cell Sci. 2002; 115:3861–3. [PubMed: 12244123]

Pearlstein E. Substrate activation of cell adhesion factor as a prerequisite for cell attachment. Int J Cancer. 1978; 22:32–35. [PubMed: 681024]

Petersen, TE.; Skorstengaard, K.; Vibe-Pedersen, K. Primary structure of fibronectin. In: Mosher, DF., editor. Fibronectin. New York: Academic Press; 1989.

Pickford AR, Campbell ID. NMR studies of modular protein structures and their interactions. Chemical reviews. 2004; 104:3557–66. [PubMed: 15303827]

Pickford AR, Potts JR, Bright JR, Phan I, Campbell LD. Solution structure of a type 2 module from fibronectin: implications for the structure and function of the gelatin-binding domain. Structure. 1997; 5:359–370. [PubMed: 9083105]

Pickford AR, Smith SP, Staunton D, Boyd J, Campbell ID. The hairpin structure of the $^{6}$F1$^{1}$F2$^{2}$F2 fragment from human fibronectin enhances gelatin binding. EMBO J. 2001; 20:1519–1529. [PubMed: 11285216]

Potts JR, Bright JR, Bolton D, Pickford AR, Campbell ID. Solution structure of the N-terminal F1 module pair from human fibronectin. Biochemistry. 1999; 38:8304–8312. [PubMed: 10387076]

Potts JR, Campbell ID. Structure and function of fibronectin modules. Matrix Biol. 1996; 15:313–320. [PubMed: 8981327]

Potts JR, Phan I, Williams MJ, Campbell ID. High-resolution structural studies of the factor XIIIa crosslinking site and the first type 1 module of fibronectin. Nature Struct Biol. 1995; 2:946–950. [PubMed: 7583666]

Rocco M, Carson M, Hantgan R, Mcdonagh J, Hermans J. Dependence of the shape of the plasma fibronectin molecule on solvent composition. Ionic strength and glycerol content. J Biol Chem. 1983; 258:14545–9. [PubMed: 6643501]

Rocco M, Infusini E, Daga MG, Gogioso L, Cuniberti C. Models for fibronectin. EMBO J. 1987; 6:2343–2349. [PubMed: 3665879]

Rudino-Pinera E, Ravelli RB, Sheldrick GM, Nanao MH, Korostelev VV, Werner JM, Schwarz-Linek U, Potts JR, Garman EF. The solution and crystal structures of a module pair from the Staphylococcus aureus-binding site of human fibronectin--a tale with a twist. Journal of molecular biology. 2007; 368:833–44. [PubMed: 17368672]

Schor SL, Ellis I, Banyard J, Schor AM. Motogenic activity of IGD-containing synthetic peptides. J Cell Sci. 1999; 112(Pt 22):3879–88. [PubMed: 10547349]

Schwarz-Linek U, Hook M, Potts JR. Fibronectin-binding proteins of gram-positive cocci. Microbes and infection / Institut Pasteur. 2006; 8:2291–8. [PubMed: 16782385]

Schwarz-Linek U, Pilka ES, Pickford AR, Kim JH, Hook M, Campbell ID, Potts JR. High affinity streptococcal binding to human fibronectin requires specific recognition of sequential F1 modules. J Biol Chem. 2004; 279:39017–25. [PubMed: 15247227]

Schwarz-Linek U, Werner JM, Pickford AR, Gurusiddappa S, Kim JH, Pilka ES, Briggs JA, Gough TS, Hook M, Campbell ID, Potts JR. Pathogenic bacteria attach to human fibronectin through a tandem beta-zipper. Nature. 2003; 423:177–81. [PubMed: 12736686]

Schwarzbauer JE. Identification of the fibronectin sequences required for assembly of a fibrillar matrix. J Cell Biol. 1991; 113:1463–1473. [PubMed: 2045422]

Sharma A, Askari JA, Humphries MJ, Jones EY, Stuart DI. Crystal structure of a heparin- and integrin-binding segment of human fibronectin. EMBO J. 1999; 18:1468–1479. [PubMed: 10075919]

Singh P, Carraher C, Schwarzbauer JE. Assembly of fibronectin extracellular matrix. Annu Rev Cell Dev Biol. 2010; 26:397–419. [PubMed: 20690820]

Smith BO, Downing AK, Dudgeon TJ, Cunningham M, Driscoll PC, Campbell ID. Secondary structure of fibronectin type 1 and epidermal growth factor modules from tissue-type plasminogen activator by nuclear magnetic resonance. Biochemistry. 1994; 33:2422–9. [PubMed: 8117702]

Smith DE, Mosher DF, Johnson RB, Furcht LT. Immunological identification of two sulfhydryl-containing fragments of human plasma fibronectin. J Biol Chem. 1982; 257:5831–5838. [PubMed: 6175633]

Smith ML, Gourdon D, Little WC, Kubow KE, Eguiluz RA, Luna-Morris S, Vogel V. Force-induced unfolding of fibronectin in the extracellular matrix of living cells. PLoS Biol. 2007; 5:e268. [PubMed: 17914904]

Smith SP, Hashimoto Y, Pickford AR, Campbell ID, Werner JM. Interface characterization of the type II module pair from fibronectin. Biochemistry. 2000; 39:8374–81. [PubMed: 10913243]

Sottile J, Hocking DC. Fibronectin polymerization regulates the composition and stability of extracellular matrix fibrils and cell-matrix adhesions. Mol Biol Cell. 2002; 13:3546–59. [PubMed: 12388756]

Sottile J, Schwarzbauer J, Selegue J, Mosher DF. Five type I modules of fibronectin form a functional unit that binds to fibroblasts and Staphylococcus aureus. J Biol Chem. 1991; 266:12840–12843. [PubMed: 1677003]

Sottile J, Shi F, Rublyevska I, Chiang HY, Lust J, Chandler J. Fibronectin-dependent collagen I deposition modulates the cell response to fibronectin. American journal of physiology Cell physiology. 2007; 293:C1934–46. [PubMed: 17928541]

Spitzfaden C, Grant RP, Mardon HJ, Campbell ID. Module-module interactions in the cell binding region of fibronectin: stability, flexibility and specificity. Journal of molecular biology. 1997; 265:565–79. [PubMed: 9048949]

Sticht H, Pickford AR, Potts JR, Campbell ID. Solution structure of the glycosylated second type 2 module of fibronectin. Journal of molecular biology. 1998; 276:177–87. [PubMed: 9514732]

Stine JM, Sun Y, Armstrong G, Bowler BE, Briknarova K. Structure and unfolding of the third type III domain from human fibronectin. Biochemistry. 2015; 54:6724–33. [PubMed: 26517579]

Stultz CM. Localized unfolding of collagen explains collagenase cleavage near imino-poor sites. Journal of molecular biology. 2002; 319:997–1003. [PubMed: 12079342]

Takagi J, Strokovich K, Springer TA, Walz T. Structure of integrin alpha5beta1 in complex with fibronectin. The EMBO journal. 2003; 22:4607–15. [PubMed: 12970173]

Takahashi S, Leiss M, Moser M, Ohashi T, Kitao T, Heckmann D, Pfeifer A, Kessler H, Takagi J, Erickson HP, Fassler R. The RGD motif in fibronectin is essential for development but

dispensable for fibril assembly. The Journal of cell biology. 2007; 178:167–78. [PubMed: 17591922]

Tamkun JW, Hynes RO. Plasma fibronectin is synthesized and secreted by hepatocytes. The Journal of biological chemistry. 1983; 258:4641–7. [PubMed: 6339502]

Tomasini-Johansson B, Mosher DF. Plasma fibronectin concentration in inbred mouse strains. Thrombosis and haemostasis. 2009; 102:1278–80. [PubMed: 19967162]

Tomasini-Johansson BR, Annis DS, Mosher DF. The N-terminal 70-kDa fragment of fibronectin binds to cell surface fibronectin assembly sites in the absence of intact fibronectin. Matrix Biol. 2006; 25:282–93. [PubMed: 16567085]

Tomasini-Johansson BR, Kaufman NR, Ensenberger MG, Ozeri V, Hanski E, Mosher DF. A 49-residue peptide from adhesin F1 of *Streptococcus pyogenes* inhibits fibronectin. J Biol Chem. 2001; 276:23430–23439. [PubMed: 11323441]

Tompa P, Schad E, Tantos A, Kalmar L. Intrinsically disordered proteins: emerging interaction specialists. Current opinion in structural biology. 2015; 35:49–59. [PubMed: 26402567]

Tooney NM, Mosesson MW, Amrani DL, Hainfeld JF, Wall JS. Solution and surface effects on plasma fibronectin structure. J Cell Biol. 1983; 97:1686–92. [PubMed: 6417145]

Tucker RP, Chiquet-Ehrismann R. Evidence for the evolution of tenascin and fibronectin early in the chordate lineage. Int J Biochem Cell Biol. 2009; 41:424–34. [PubMed: 18761101]

Ugarova TP, Zamarron C, Veklich Y, Bowditch RD, Ginsberg MH, Weisel JW, Plow EF. Conformational transitions in the cell binding domain of fibronectin. Biochemistry. 1995; 34:4457–4466. [PubMed: 7535564]

Vakonakis I, Staunton D, Ellis IR, Sarkies P, Flanagan A, Schor AM, Schor SL, Campbell ID. Motogenic sites in human fibronectin are masked by long range interactions. J Biol Chem. 2009; 284:15668–75. [PubMed: 19366708]

Vakonakis I, Staunton D, Rooney LM, Campbell ID. Interdomain association in fibronectin: insight into cryptic sites and fibrillogenesis. The EMBO journal. 2007; 26:2575–83. [PubMed: 17464288]

Velling T, Risteli J, Wennerberg K, Mosher DF, Johansson S. Polymerization of type I and III collagens is dependent on fibronectin and enhanced by integrins alpha 11beta 1 and alpha 2beta 1. J Biol Chem. 2002; 277:37377–81. [PubMed: 12145303]

Wang Y, Reheman A, Spring CM, Kalantari J, Marshall AH, Wolberg AS, Gross PL, Weitz JI, Rand ML, Mosher DF, Freedman J, Ni H. Plasma fibronectin supports hemostasis and regulates thrombosis. J Clin Invest. 2014; 124:4281–93. [PubMed: 25180602]

White ES, Baralle FE, Muro AF. New insights into form and function of fibronectin splice variants. J Pathol. 2008; 216:1–14. [PubMed: 18680111]

Williams EC, Janmey PA, Ferry JD, Mosher DF. Conformational states of fibronectin. Effects of pH, ionic strength, and collagen binding. J Biol Chem. 1982; 257:14973–14978. [PubMed: 7174679]

Williams MJ, Phan I, Harvey TS, Rostagno A, Gold L, Campbell ID. Solution structure of a pair of fibronectin type 1 modules with fibrin binding activity. J Mol Biol. 1994; 235:1302–1311. [PubMed: 8308892]

Xu J, Maurer LM, Hoffmann BR, Annis DS, Mosher DF. iso-DGR sequences do not mediate binding of fibronectin N-terminal modules to adherent fibronectin-null fibroblasts. J Biol Chem. 2010; 285:8563–71. [PubMed: 20097751]

Yi M, Ruoslahti E. A fibronectin fragment inhibits tumor growth, angiogenesis, and metastasis. Proceedings of the National Academy of Sciences of the United States of America. 2001; 98:620–4. [PubMed: 11209058]

Yi M, Sakai T, Fassler R, Ruoslahti E. Antiangiogenic proteins require plasma fibronectin or vitronectin for in vivo activity. Proceedings of the National Academy of Sciences of the United States of America. 2003; 100:11435–8. [PubMed: 13679585]

Zerlauth G, Wolf G. Plasma fibronectin as a marker for cancer and other diseases. Am J Med. 1984; 77:685–9. [PubMed: 6385694]

Zhang Q, Checovich WJ, Peters DM, Albrecht RM, Mosher DF. Modulation of cell surface fibronectin assembly sites by lysophosphatidic acid. J Cell Biol. 1994; 127:1447–1459. [PubMed: 7962101]

Zhang Q, Mosher DF. Crosslinking of the N-terminal region of fibronectin to molecules of large apparent molecular mass (LAMMs): Characterization of fibronectin assembly sites induced by the treatment of fibroblasts with lysophosphatidic acid. J Biol Chem. 1996; 271:33284–33292. [PubMed: 8969187]

Zhou X, Rowe RG, Hiraoka N, George JP, Wirtz D, Mosher DF, Virtanen I, Chernousov MA, Weiss SJ. Fibronectin fibrillogenesis regulates three-dimensional neovessel formation. Genes & development. 2008; 22:1231–43. [PubMed: 18451110]

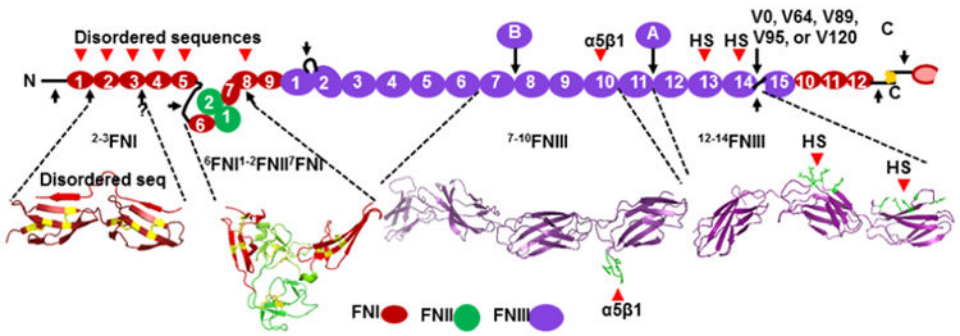


**Fig. 1.**

Model of FN subunit. One subunit of a FN dimer is displayed with FNI modules, FNII modules, and FNIII modules numbered as they are ordered from N- to C-termini. Locations of alternatively spliced $^{A}$FNIII (A) and $^{B}$FNIII (B) FNIII modules, when present, are indicated. Alternative splicing also results in five different sequences for the variable (V) region, labeled by the number of amino acids (V0, V64, V89, V95, or V120). Subunits of FN are connected by a brace of disulfide bonds at the extreme C-termini. Crystal structures of $^{2\text{-}3}$FNI (PDB 2RKZ), $^{6\text{-}7}$FNI (PDB 3MQL), $^{7\text{-}10}$FNIII (PDB 1FNF), and $^{12\text{-}14}$FNIII (PDB 1FNH) are shown below the display of the subunit. Structures have been manipulated by PyMOL (https://www.pymol.org) to emphasize features discussed in the review. The nomenclature used to designate arrays of modules in the figure is used throughout. Sites of interactions with disordered sequences of bacterial adhesins, α5β1 integrin, and heparan sulfate (HS) are indicated by arrowheads with sidechains interacting with α5β1 or heparan sulfate colored green. The crystal structure of $^{2\text{-}3}$FNI is shown with a peptide from a bacterial adhesion bound by anti-parallel β-strand addition. Likely stretches of disordered sequences (thick lines) within FN itself or sites of heightened flexibility between consecutive FN modules are indicated by arrows. A color version of the figure is available online in which type I, II, and III FN modules are red, green, and purple, respectively; disulfides are yellow; interacting side chains are green; and arrowheads are red.

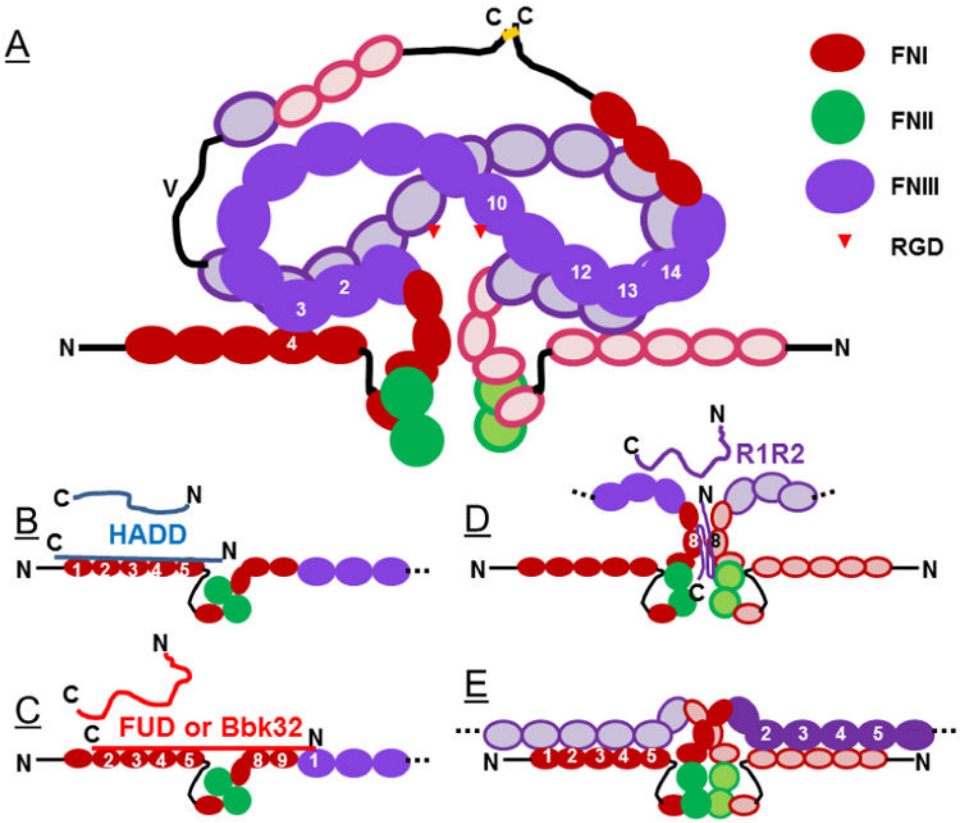


**Fig. 2.**

Models of the quaternary structure of globular dimeric plasma FN (A), how the structure may be altered by interaction with polypeptides based on the high affinity downstream domain (HADD) or functional upstream domain (FUD) of the F1 adhesin of *S. pyogenes* or the Bbk32 segment of BBK32 of *B. burgorferi* (B, C) or the R1R2 tandem repeats of *S. equis* subspecies *equis* (D), and how FN may interact to form fibrils in extracellular matrix (E). Color scheme and abbreviations are as for Fig. 1. Modules in one subunit are in solid whereas those of the opposite subunits are lighter and outlined. Arrowheads indicate the locations of RGD sequences in $^{10}$FNIII modules recognized by α5β1 integrin. As described in the text, the globular quaternary structure and cryptic state of $^{10}$FNIII are proposed to be favored by intra-subunit interactions between $^{4}$FNI and $^{3}$FNIII and inter-subunit interactions between $^{2\text{-}3}$FNIII and $^{12\text{-}14}$FNIII (A). The adhesin-derived polypeptides are depicted as being unstructured when unbound and interacting with specific FN modules by anti-parallel β-strand addition. Displacement of $^{3}$FNIII from $^{4}$FNI by HADD, FUD, or Bbk32 (B, C) is depicted as causing elongation of individual FN subunits whereas binding or R1R2 is favored by the compact conformation and ability to ligate both subunits. Panel E is highly schematic and should be compared to a similar schematic referenced in the text. A color version of the figure is available online in which type I, II, and III FN modules are red, green, and purple, respectively.